www.ptcer.pl/mccm

MATERIAŁY CERAMICZNE /CERAMIC MATERIALS/, 62, 3, (2010), 301-306

Analysis of Residual Stresses Using the $\sin^2\psi$ Method for Al_2O_3 Materials before and after Grinding and Heat Treatment Processes

P. Putyra[1]*, S. Skrzypek[2], B. Smuk[1], M. Podsiadło[1]

[1] Institute of Advanced Manufacturing Technology, Kraków, Poland
[2] AGH University of Science and Technology, Faculty of Metals Engineering and Industrial Computer Science, Kraków, Poland
*e-mail: piotr.putyra@ios.krakow.pl

Abstract

This work presents the results of analysis of residual stresses generated at various stages of production of Al_2O_3 sinters (sintering, mechanical processing). Residual stresses were determined by the g-$\sin^2\psi$ X-ray method. The process of ceramic sintering of Al_2O_3 was carried out at varying parameters: temperature and heating time, heating rate, cooling rate. After mechanical processing (grinding), the materials were subjected to heat treatment, consisting of heating to temperatures in the range of 600–1200°C. In order to determine the mechanical properties of the materials, *HV30*, *HV0.3* and *HV0.1* hardness measurements were made. K_{Ic} and HVG stress intensity index values were also determined.

Keywords: Residual stresses, Al_2O_3, Mechanical properties, g-$\sin^2\psi$ method

ANALIZA NAPRĘŻEŃ RESZTKOWYCH ZA POMOCĄ METODY $\sin^2\Psi$ W MATERIAŁACH Al_2O_3 PRZED I PO PROCESACH SZLIFOWANIA I OBRÓBKI CIEPLNEJ

W pracy zaprezentowano wyniki analizy naprężeń resztkowych powstających na różnych etapach produkcji spieków Al_2O_3 (spiekanie, obróbka mechaniczna). Naprężenia resztkowe oznaczono rentgenowską metodą g-$\sin^2\psi$. Spiekanie ceramiki Al_2O_3 przeprowadzono przy zróżnicowanych parametrach procesu: temperatura i czas ogrzewania, szybkość ogrzewania i studzenia. Po obróbce mechanicznej (szlifowanie) materiały poddano obróbce cieplnej polegającej na ogrzewaniu do temperatury z zakresu 600–1200°C. Aby określić właściwości mechaniczne zmierzono twardość *HV30*, *HV0.3* i *HV0.1* materiałów. Oznaczono też wartości współczynników intensywności naprężeń K_{Ic} i HVG.

Słowa kluczowe: naprężenia resztkowe, Al_2O_3, właściwości mechaniczne, metoda g-$\sin^2\psi$

1. Introduction

Residual stresses belong to the most significant technological problems both in the production and in the use of ceramic materials. Residual stresses, and subsequently cracks arising as a result of the appearance of temperature gradients during sintering (thermal stresses) and as a result of mechanical processing, may have the effect on lowering the strength of ceramic pieces [1-5].

Thermal stresses appear mainly in multiphase ceramic materials [6-8] and ceramic-metal composites [9]. Methods of determining and modelling thermal stresses in multiphase materials have been the subject of many studies and are described quite extensively in the literature [9, 10]. However, taking into account the anisotropy of thermal conduction and the anisotropy of linear expansion of certain ceramic materials, residual stresses may also appear in single-phase materials [11]. Grains of various phases, or of various linear expansion coefficients are the cause of deformations and stresses. A significant characteristic of these stresses is their appearance and counteraction in zones, in a row of several adjacent grains. Besides residual stresses of a thermal nature in single- and multi-phase materials, it is also possible to produce a state of stress as a result of mechanical processing.

Mechanical processing of ceramic materials, regardless their hardness and brittleness, may take place as a result of grinding in the conditions of ductile material removal or of grinding in the conditions of brittle material removal. The conditions of ductile material removal are ensured when the load of the abrasive grain does not exceed the threshold values or appropriate threshold penetration depth of the abrasive grain in the material. Over and above these values, the dominant mechanism of material removal is brittle cracking [12]. The energy required for brittle cracking is proportional to the square of the penetration depth of the abrasive grain in the material, whilst the energy required for plastic deformation is proportional to the cube of this depth [4]. The

relation between the plastic deformation energy and the brittle cracking energy is therefore proportional to the value of penetration depth of the abrasive grain in the material. As the range of processing decreases, plastic deformation becomes (from an energy point of view) a more advantageous mechanism for the separation of material. The appearance of cracking as a result of grinding particularly lowers the tensile strength of ceramic pieces. The theory of the action of notches in stretching explains the reduction in strength as a result of the appearance of cracks in the top layer, and the concentration of stresses at the base of the notch may initiate the propagation of cracks. In the case of grinding in conditions of plastic material removal, the arising residual stresses affect the strength properties of ceramic materials, which is result from both the fact of their size and superposition with stresses from external (operational) loads. The introduction of compression stresses to the surface layer of ceramic materials in the course of mechanical processing prompts a significant increase in surface resistance to cracking and microhardness [13].

The aim of this study was to determine residual stresses and their effects on selected properties of ceramic materials (chiefly hardness and resistance to brittle cracking) at various production stages of sinters and at various selection of heat treatment parameters after mechanical processing.

The scope of this study encompasses the determination of residual stresses generated during sintering, mechanical processing or heat treatment). Individual sintering processes were carried out with various parameters at diverse rates of heating and cooling of the charge and duration of heating at maximum temperature. After mechanical processing, ceramic samples were subjected to heat treatment, consisting of heating to temperatures ranging from 600°C to 1200°C. As a part of the study, *HV30*, *HV0.3* and *HV0.1* hardness measurements were made, and K_{Ic} stress intensity index values were determined. Residual stresses were determined by the g-sin$^2\psi$ method [14, 15] and by EBSD electron backscatter diffraction detection.

2. Experimental

2.1. Material for Analysis

Al_2O_3 powder (ALCOA CT3000SG) of an average particle size of 0.7 μm, containing 0.3 % MgO powder (Reachim, FLUKA) of a particle size in the range of 0.5–1 μm and 5 % Polyethylene Glycol 400, was used.

Individual mixtures were prepared in a colloid mill, then granulated using a sieve with a mesh size of 0.9 mm. Pressing was carried out in an uniaxial steel die at a pressure of 110 MPa and isostatic densification at a pressure of 250–300 MPa. After first being dried with a programmed temperature increase to 210°C, the compacts were sintered in a Nabertherm furnace.

Sample sintering process parameters:

S-1 – heating at 1615°C for 60 minutes; slow cooling at a rate of 5°C/min.

S-2 – heating at 1550°C for 300 minutes; slow cooling at a rate of 5°C/min.

S-3 – heating at 1550°C for 180 minutes; slow cooling at a rate of 5°C/min.

S-4 – heating at 1550°C for 120 minutes; slow cooling at a rate of 5°C/min.

S-5 – heating at 1615°C for 60 minutes; rapid cooling.

Due to a macroscopic temperature gradient, both in heating and in cooling, and on account of the low thermal conduction coefficients of ceramic materials, significant thermal residual stress states appear. The appearance of residual stresses of the second kind, particularly in Al_2O_3-based ceramics, results from anisotropy of thermal conduction and anisotropy of linear expansion. In the case of a hexagonal (trigonal) system, the thermal conduction tensor has two main coefficients, $\lambda_{11} = \lambda_{22}$ and λ_{33}. The relationship between the main thermal conduction coefficients for Al_2O_3 corundum crystallizing in a hexagonal system is $\lambda_{11}/\lambda_{33} = 0.85$ [16].

Materials sintered according to parameters S-1 were then subjected to grinding. Abrasive machining was carried out using a diamond abrasive wheel (AC 6 diamond grain of granulation D 107) on SS-200/B-type stands designed and manufactured at IOS. The circumferential grinding speed used was in the range of v_c = 15–18 m/s and radial feed speed v_{fr} = 10 mm/s; cross (axial) feed was controlled manually. Further information on the parameters of the polishing process is contained in Ref. [17].

After mechanical processing, the samples were subjected to heat treatment for relaxation of stresses generated during polishing. The materials were heated at various temperatures, the process itself being carried out according to temperature curves, corresponding to the following:

HT-1 – heating at 600°C for 30 minutes; slow cooling with furnace.

HT-2 – heating at 800°C for 30 minutes; slow cooling with furnace.

HT-3 – heating at 1000°C for 30 minutes; slow cooling at a rate of 3°C/min.

HT-4 – heating at 1200°C for 30 minutes; slow cooling at a rate of 3°C/min.

2.2. Measurement Methodology

Apparent density, ρ_p, was measured by the hydrostatic method. Microstructure analysis of the composites was carried out using a JEOL JSM 6460LV scanning microscope equipped with an EBSD spectrometer for electron backscatter detection. On account of the lack of electrical conduction of the samples studied, observations were made under conditions of reduced vacuum. Hardness was determined by the Vickers method at loads of 294.2 N, 2942 mN and 980.7 mN, using a Frankoskop hardness tester and a Future Tech. Corp. FM-7 digital microhardness tester. Metallographic specimens were prepared for these studies using Struers equipment and polishing media. Young's modulus measurements were also made for the sintered samples using the ultrasound method for measurement of passing speed of transverse and longitudinal waves using a Panametrics Epoch III flaw detector. The Vickers indentation method was used to measure the lengths of cracks around the impression in the sample, made with an indenter load force of 294.2 N, and then calculated using a Niihara model coefficient of resistance to brittle cracking (K_{Ic}) [3,18].

In order to reveal stresses of the second kind (arising as the result of varying temperature expansions in individual

areas of the sample), measurements were made both on the surface and in the central area. Differences of expansion in individual areas (particularly at short heating and sintering times) are the result of heterogeneous heating of the sample volume. Hardness measurements at the lower load of 294.2 N (*HV0.3*) for individual samples (on the surface and in the central area) were supposed to reveal the appearance in the material of stresses of the second kind. However, taking into account that the analysed materials were distinguished by a fine-grained microstructure, additional hardness measurements were carried out at an indenter load force of 980.7 mN (*HV0.1*). Due to limitations in the measurement of diagonal length of impressions, measurements were not made at loads of less than 980 mN.

In order to analyse precisely the internal stresses in the material after sintering, after mechanical processing and after heat treatment, Al_2O_3-based ceramic materials were subjected to measurement of macroscopic residual stresses using the diffractometric method. The use of the Bragg equation for precise calculation of distances between crystallographic planes enables the measurement of plastic deformation and, through this, the measurement of macroscopic stresses acting on the crystal structure in the range of linear elasticity.

The value of internal stresses was determined by the g-$\sin^2\psi$ method, worked out by Skrzypek [14, 15], using diffraction in grazing-incidence angle geometry (grazing-incidence angle X-ray diffraction). The g-$\sin^2\psi$ method combines Hooke's equation for a plane state of stresses defined in the sample coordinate system as *S* with components of deformation in the measurement system *L* (Fig. 1).

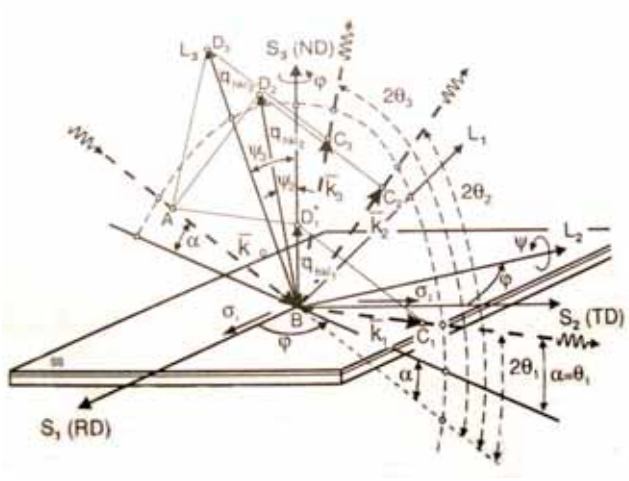

Fig. 1. Spatial system of a beam falling and diffracted by three reflections {hkl} in diffraction at a fixed angle of incidence and component stresses on the surface in sample coordinate system, S_i, and measurement system, L_j. Orientation of diffraction vectors for three selected plane groups {hkl} is denoted by q_{hkl} [14].

The basic equation of this method, assuming a plane state of stresses, takes the form of a linear relationship $\varepsilon_{rtg}=f(\sin^2\psi)$ (Fig. 2) and is used for calculations of residual macrostresses. In the case of more complex structures (e.g. tetragonal, hexagonal) it is necessary to use the tetragonal/hexagonal index *c/a*. For calculations of absolute values, $\sigma\varphi$, measurement of the interplanar distance of the standard material (without stresses) is not necessary, as stress is calculated in a straight line.

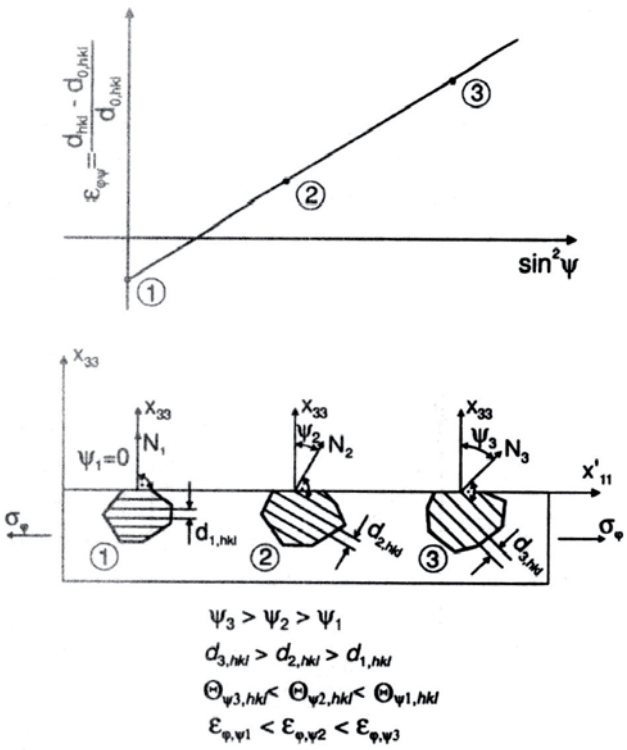

Fig. 2. Linear relationship $\varepsilon^L_{\varphi\psi} = f(\sin^2\psi)+b$. Points (1), (2) and (3) indicate measurements of distance between planes {hkl} in appropriately oriented grains of the microstructure [14].

In order to reveal residual stresses resulting from mechanical processing, Al_2O_3-based material was also subjected to analysis using a scanning microscope combined with EBDS electron backscatter diffraction detection. In the scanning microscope, a convergent beam of electrons interacts with the sample inclined toward the electronoptical axis, as a result the electrons undergo diffraction (in accordance with Bragg's law) on crystallographic planes in the superficial layers of the analysed material (to a depth of 50 nm). On the assumption that residual stresses have an effect on the change in interplanar distances in crystallographic grains, areas of unresolved electron backscatter diffraction may represent their appearance.

First, sample analyses were carried out without surface preparation. Samples were observed at 2000x magnification and under conditions of reduced vacuum. Then, analyses were carried out on the samples whose observation surfaces had been prepared by polishing. Struers RotoPol-21 polishers and diamond suspensions of average powder size 3 mm were used in preparation of the surfaces. EBSD analysis of the surfaces of individual samples after polishing was carried out at 2000x and 5000x magnification. All analyses were carried out indexing a minimum of 4 planes, with a measurement error of max. 2°. The measurement error is defined by the angle deviation between the actual arrangement of Kikuchi bands and that generated by the index program.

3. Results of analysis

3.1. Mechanical properties of Al_2O_3 materials

Presented in Table 1 are the results of measurements of density and hardness, and calculated stress intensity

index values, obtained for Al_2O_3-based ceramics, according to sintering profile.

3.2. Mechanical properties of Al_2O_3 materials after polishing and after heat treatment

Samples, after sintering, after polishing and after various heat treatment processes, were subjected to hardness measurements (*HV0.3*, *HV0.1* and *HV30*) and K_{Ic} stress intensity index value was determined. The results of these examinations are compared in Table 2. Hardness and resistance to cracking were determined for samples after sintering S-1, after polishing and after heat treatment. In order to determine the effect of cooling rate from sintering temperature, hardness and stress intensity index value were also determined for samples after sintering S-5.

3.3. Analysis of residual stresses by X-ray diffraction

Values of residual macrostresses, determined using the g-sin$^2\psi$ X-ray method [14, 15], are presented in Table 3 and in graphic form in Fig. 3. Estimation error was in the range of 5-10 % of values given. Labelling of samples: Sample 1 (after sintering S-1); Sample 2 (after sintering S-1 and after grinding); Sample 3 (after sintering S-1, grinding and heat treatment HT-4).

3.4. Structural Investigations

Materials after sintering, after polishing and after heat treatment at a temperature of 1200°C were subjected to observation under a scanning microscope at a magnification of 2000x and 5000x respectively. On account of corundum ceramic being an isolator, observations under the scanning microscope were carried out under the conditions of reduced vacuum of 15 Pa. is An example microstructure of samples after sintering S-1, and subjected to mechanical processing is presented in Fig. 4 and Fig. 5, respectively.

3.5. Electron backscatter diffraction analysis

The results of electron backscatter diffraction analysis of samples after sintering, after mechanical processing and after heat treatment (1200°C) are presented in Table 6.

Table 1. Comparison of measurement results of density, Young's modulus, hardness (HV0.3, HV30) and calculated K_{Ic} stress intensity index values.

Sintering	Young's modulus [GPa]	ρ_p [g/cm^3]	Point of measurement	*HV30*	SD	*HV0.3*	SD	K_{Ic}	SD
S-1	386	3.90	surface	1594	23	1720	261	2.61	0.09
			centre	1567	33	1837	87	2.70	0.08
S-2	379	3.85	surface	1613	16	1812	100	2.55	0.09
			centre	1594	20	1889	71	2.53	0.07
S-3	378	3.85	surface	1618	16	1851	111	2.58	0.22
			centre	1608	18	1922	73	2.58	0.05
S-4	373	3.83	surface	1606	17	1884	64	2.56	0.08
			centre	1619	27	1719	63	2.58	0.08
S-5	383	3.91	surface	1603	26	1756	120	2.57	0.07
			centre	1597	10	1815	52	2.59	0.05

Table 2. Comparison of measurement results of hardness (HV0.3, HV0.1, HV30) and K_{Ic}.

State				*HV30*	SD	*HV0.3*	SD	*HV0.1*	SD	K_{Ic}	SD
Sintering			S-1	1564	57	1857	52	2070	103	2.59	0.04
			S-5	1597	10	1815	52	1891	38	2.59	0.05
	Polishing			1569	19	1830	88	1967	104	2.62	0.05
		Heat treatment	HT-1	1590	31	1776	41	1857	95	2.60	0.06
			HT-2	1586	30	1770	35	1876	99	2.61	0.09
			HT-3	1576	52	1791	39	1940	33	2.66	0.10
			HT-4	1594	28	1815	40	1894	59	2.57	0.06

Table 3. Comparison of measurement results of residual macrostresses using the g-sin$^2\psi$ X-ray method.

Depth [μm]	Residual stress value [MPa]		
	Sample 1	Sample 2	Sample 3
0-2	+270	+230	+390
3-5	+160	-450	+200
6-8	+50	-800	+60
12-15	0	-590	0

Table 4. Comparison of results of electron backscatter diffraction analysis. Share of surface with diffractions.

Sample state	Surface state	Mag.	Resolved	Unresolved
Sintering	raw	2000x	71.5	28.5
	polished	2000x	72.7	27.3
		5000x	83.3	16.7
Sintering Grinding	raw	2000x	33.7	66.3
	polished	2000x	62.3	37.7
		5000x	84.1	15.9
Sintering Grinding Heat Treatment	raw	2000x	46.4	53.6
	polished	2000x	80.8	19.2
		5000x	85.3	14.7
Area around *HV30* indentation	polished	2000x	47.2	52.8
		5000x	49.3	50.7

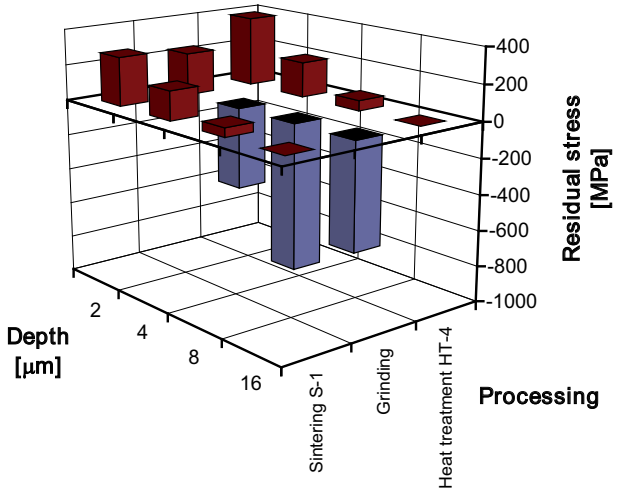

Fig. 3. Residual stress values, determined using the g-$\sin^2\psi$ X-ray method, in Al_2O_3 samples, resulting from sintering, mechanical processing (grinding), and heat treatment at a temperature of 1200°C after grinding.

Presented are the shares of the surface for which indexing of individual crystallographic planes was possible, according to the range of processing of the ceramic samples (sintering, mechanical processing, heat treatment) and according to the state of the analysed surface (raw, polished, deformed).

In order to emphasise the effect of residual stresses in the superficial layers, an analysis was also carried out of the surface in the area of the HV30 impression. The impression was made in the sample after mechanical processing, whose surface was prepared by polishing.

4. Discussion

In the course of these studies, no significant differences were found in *HV30* hardness values for Al_2O_3 materials after various variants of sintering. Impressions made at a load of 292.4 N were to serve to define K_{Ic} stress intensity index values for individual materials. In the case of Al_2O_3-based ceramics, calculated K_{Ic} values in the surface layer and in the central layer reveal no significant differences, irrespective of the cooling rate of individual samples. On the basis of these

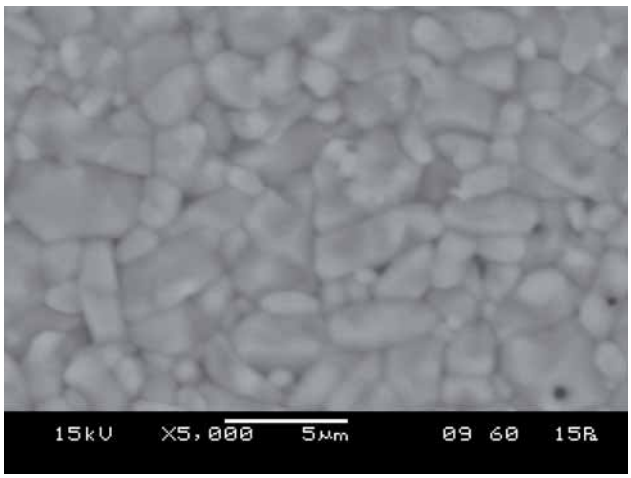

Fig. 4. Microstructure of Al_2O_3 samples after sintering.

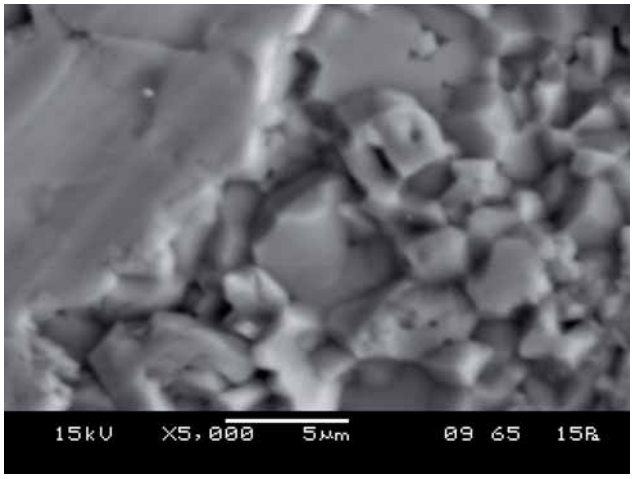

Fig. 5. Microstructure of Al_2O_3 after grinding.

studies, the effect of residual stresses in the superficial layers on the resistance stress intensity index value was not confirmed. Taking into account that the depth and diameter of the Vickers impression at a load of 292.4 N significantly exceed the range of appearance of residual stresses, a correlation between residual stress value and resistance to cracking might be revealed using a smaller load. On the basis of differences in *HV0.3* hardness measured in the central area and on the surface of Al_2O_3 samples, one may deduce the appearance of residual stresses of the third kind. The large distribution of *HV0.1* values measured on identical surfaces of suitable samples testifies to the appearance of stresses, which encompass in their range several crystallites (residual stresses of the second kind). The possible appearance of stresses of the second kind is testified by the fact that the diameter of the impression at a load force of 980.7 mN usually encompasses from several up to twenty grains.

The appearance of macroscopic residual stresses was confirmed as a result of X-ray examinations. On the basis of these studies, the appearance was found, in the surface layer of samples after sintering, of tensile stresses of values not exceeding 300 MPa. At a depth of up to 8 mm from the surface of the sample, the value of these stresses fell to 50 MPa. Residual stresses of the same sign were also calculated in the case of samples which after polishing were

subjected to heat treatment at a temperature of 1200°C. Both the value and the range of appearance of these tensions were similar for samples after sintering and after heat treatment. In the case of samples after polishing, the value and range of calculated stresses were completely different. It may be stated that as a result of mechanical processing, compressive stresses are dominant in the material, whose values amount to as much as 800 MPa. Also, the range of appearance of tensions generated as a result of mechanical processing is greater than that of tensions generated as a result of heat treatment or sintering. The sample after polishing, at a depth of 15 mm from the surface, was characterised by compressive stresses, whose values exceeded 500 MPa. It should be added here that, according to the angle of incidence of the beam, the width of the area in which diffraction appears covers several mm^2. A beam of width 0.1 mm at an angle of incidence of α = 1° irradiates a surface of width 5.7 mm. Internal stresses recorded using the g-$\sin^2\psi$ X-ray method may be counted as stresses of the first kind, arising as the result of a temperature gradient or plastic deformation. Analysing the surface appearance of samples after polishing, it may be stated that mechanical processing took place both in conditions of ductile and of brittle material removal. Traces of plastic deformation and areas in which intercrystalline is dominant are well visible. On the basis of these studies, it may be demonstrated that the use of mechanical processing introduces into the top layer of corundum ceramic compressive stresses of 800 MPa. With the polishing parameters used, it was not, however, possible to obtain a surface free of crumbling or cracking. In this case, it is necessary to optimise mechanical processing parameters so that the generation of compressive stresses in the superficial layers would not be accompanied by a loss of cohesion of these layers and microcracking. The appearance of tensile stresses in the superficial layer may be explained by too rapid cooling of the ceramic samples. A temperature gradient then arises and the surface of the sample contracts more quickly than the inside of the material. The temperature gradient which arises is not, however, so large that the thermal shock resulting from cooling initiates stable cracking.

Residual stresses were also revealed as a result of analyses carried out using the EBSD method. Analysing EBSD quality maps, it may be stated that the residual stresses that appear encompass, a row of several adjacent grains in their range zones. In contrast to the stresses revealed by the X-ray method, the stresses revealed by the EBSD method may be counted as stresses of the second kind. In the case of samples after polishing of the raw surface, the share of the surface for which planes were indexed came to only 33 %. Under the same measurement conditions, the share of the surface with resolved diffractions, for samples after sintering and after heat treatment came to, respectively: 71 % and 46 %. Similar results were obtained for samples whose surfaces had been prepared by polishing. The share of the surface with resolved diffractions came to: after sintering, 72 %; after polishing, 62 %; and after heat treatment, 80 %. The effect of residual stresses on the share of the surface for which resolving diffraction is possible is revealed by the results of analysis of diffraction of electrons from the surface in the area of the *HV30* impression. The share of the surface with resolved diffractions for the sample after polishing without an impression came to 80 %, whilst this share of the surface for the sample after polishing, located in the area of the *HV30* impression, fell to 47 %.

5. Conclusions

These studies revealed that fading tensile stresses in the superficial layer arise during cooling after sintering. The thickness of the superficial layer in which stresses arise can be maximum 16 mm. The mechanical processing of sinters caused compressive stresses to arise in the superficial layer; the value and range of these stresses is significantly greater. The mechanical processing parameters used caused polishing to take place both in the conditions of ductile and of brittle material removal. With appropriate polishing parameters, it is possible to generate compressive stresses in the superficial layer without a loss of cohesion or the appearance of microcracks and tears. The use of heat treatment causes relaxation of stresses generated by polishing. It is, however, necessary to use very slow cooling. At a cooling rate of 3°C/min., stresses were found to appear in the superficial layer of the same sign, similar value and range to those stresses generated by sintering.

References

[1] Nadachowski F.: Zarys Technologii Materiałów Ogniotrwałych, Śląskie Wydawnictwo Techniczne, Katowice, 1995.
[2] Pampuch R., Błażewicz S., Górny G.: Materiały Ceramiczne dla Elektroniki, Wydawnictwa AGH, Kraków, 1993.
[3] Olszyna A.R.: Twardość a Kruchość Tworzyw Ceramicznych, Oficyna Wydawnicza Politechniki Warszawskiej, Warszawa, 2004.
[4] Oczoś K.E.: Kształtowanie Ceramicznych Materiałów Technicznych, Oficyna Wydawnicza Politechniki Rzeszowskiej, Rzeszów, 1996.
[5] Grabowski G., Stobierski L.: Ceramika/Ceramics, 91, (2005), 627-634.
[6] Bućko M.M., Pyda W.: Grabowski G., Pędzich Z., Kompozyty/Composites, 6, 3, (2006), 59-64.
[7] Pędzich Z., Grabowski G.: Kompozyty/Composites, 6, 2, (2006), 7-10.
[8] Iwaszko J.: Ceramika/Ceramics, 103, (2008), 671-678.
[9] Kaliński D., Chmielewski M.,: Ceramika/Ceramics 103, (2008), 65-72.
[10] Babski K., Boczkowska A., Konopka K., Krzesiński G., Kurzydłowski K.J.: Kompozyty/Composites, 5, 3, (2005), 40-44.
[11] Tomaszewski H.: Ceramika/Ceramics, 103, (2008), 333-348.
[12] Wszołek J., Kurleto A., Smuk B., Kasina J.: Ceramika/Ceramics, 91, (2005), 427-434.
[13] Tomaszewski H., Godwod K., Diduszko R., Carrois F., Duchazeaubeneix J.M.: Ceramika /Ceramics, 91, (2005), 451-458.
[14] Skrzypek S.J.: „Nowe Możliwości Makronaprężeń Własnych Materiałów przy Zastosowaniu Dyfrakcji Promieniowania X w Geometrii Stałego Kąta Padania", Rozprawy Monografie, AGH Uczelniane Wydawnictwa Naukowo-Dydaktyczne, Kraków, 2002.
[15] Skrzypek S.J., Baczmański A.: Adv. X-Ray Anal., 44, (2001), 134-145.
[16] Chojnacki J.: Elementy Krystalografii Chemicznej i Fizycznej, Państwowe Wydawnictwa Naukowe, Warszawa, 1971.
[17] Musiałek K., Kurleto A., Staniewicz-Brudnik B., Majewska-Albin K.: w Naukowa Szkoła Obróbki Ściernej, Gdańsk-Jurata, 1999.
[18] Niihara K., Morena R., Hasselman D.P.H.: J. Mater. Sci. Lett., 1, (1982), 13-16.

♦

Received 1 March 2010; accepted 8 May 2010